

# The science and context of accelerator driven HEDP

Richard W. Lee, LLNL

## I. Introduction

The recent increase in interest in the regime of High Energy Density (HED) Science witnessed by three broad-based scientific reports ( a) *Connecting Quarks with the Cosmos: Eleven Science Questions for The New Century* (National Academies Press, 2003); b) *Frontiers in High Energy Density Physics - The X-Games of Contemporary Science* (National Academies Press, 2003); and c) *Frontiers For Discovery In High Energy Density Physics* (prepared for National Science and Technology Council's Interagency Working Group on the Physics of the Universe, see [http://www.sc.doe.gov/production/henp/np/program/docs/HEDP\\_Report.pdf](http://www.sc.doe.gov/production/henp/np/program/docs/HEDP_Report.pdf), 2004) provides the impetus to explore the potential for the heavy ion beam community to participate in the generation of HED matter with the express purpose of improving our fundamental knowledge in this exciting regime.

The discussion below sets the stage for the proposed heavy ion beam studies that are considered. First we will provide a general background describing the regimes and physical processes of interest. This is meant to be a simple explanation of the problems of interest included for completeness and, as such, should not be considered exhaustive. Next in keeping with the goal of providing the backdrop for the proposed heavy-ion beam experiments and facilities we will outline the various aspects of HED science that are being performed currently on existing facilities. The plans for experiments on current facilities, in a general sense will also be outlined to indicate the direction of the activity in the field. Finally, we will look at the future proposed facilities to examine where a heavy ion beam proposal would be placed.

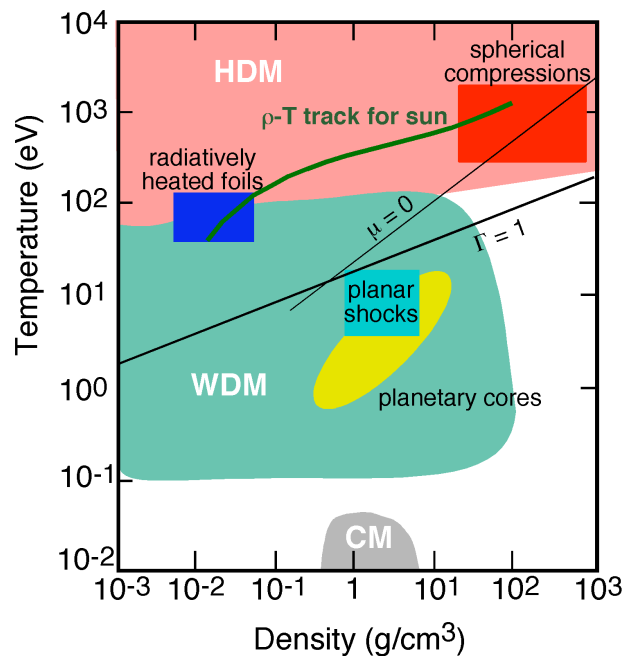


**Figure 1: Hydrogen phase diagram indicating the high energy density regime separated into the hot dense region (pink) and the warm dense region (green). Various states found in nature are indicated on the graph. The above the line  $\mu = 0$  is the region where degeneracy is unimportant, while above the line  $\Gamma = 1$  strong coupling effects are unimportant. The condensed matter phase is indicated by the gray region. The data is taken from a compilation of data from the NRL Plasma Formulary (Huba, 2000)**

The general definition of the HED regime can be illustrated by reference to the hydrogen temperature-density phase space graph in Fig. 1. Here we show the temperature–density phase space of hydrogen. The HED regime can be separated into the hot dense matter (HDM) region shown in pink and the warm dense matter (WDM) region shown in green. HDM occurs in astrophysical plasmas in supernovas, accretion disks, and stellar interiors –in Fig.1 the temperature-density track relevant to the sun is shown. Further, HED matter can be produced in laboratory-based plasma generation devices such as laser-produced plasmas and pulsed power machines, e.g., Z-pinchs. In Fig. 1 we roughly note the phase space in the HDM region occupied by the plasma produced in inertial fusion compression and foils irradiated by x-ray created at these laboratory-based facilities.

The WDM matter region, on the other hand, is a more complex object of study and will be discussed in more detail below. WDM occurs in the cores of large planets where the pressures become immense. The WDM region is accessed by all laboratory experiments that starts out as solid and end up in the plasma states; thus exploding wire arrays or laser-matter produced plasmas all transit the WDM region. Further, high-pressure shocks where the temperature becomes substantial – for shocks that is- access the WDM region. Finally, it is worth noting that in indirectly driven inertial fusion the desire to remain on a low temperature adiabat during the early phase of the compression indicates that on the run-in phase of the implosion the compressing material is in the WDM state.

It is important to understand that the usual condensed matter (CM) phase is not of interest in the HED regime. We schematically illustrate the CM matter region with the gray area at low temperature near normal density.

We will show that as a result of our analysis we believe that the heavy ion beam capability is of interest and important as it provides an alternative method to reach interesting states of matter in the HED regime. Particularly important are the contributions that such a capability will play in the Warm Dense Matter part of the HED phase space. Indeed we think that the heavy ion beams have a decided advantage in creating WDM due to several considerations: The ion beams can provide relatively large sample sizes ( $\text{mm}^3$ ); more uniform conditions; achieve high entropy at high density; the extreme conditions persist for long times; and, the repetition rates can be high. In contrast, optical laser-based experiments in WDM regime tend to have: smaller volumes; larger gradients; shorter lifetimes; and, lower repetition rates.

## II. Background

Since the late 1960's research into the regime of finite temperature matter has moved toward higher density regimes. The advent of laser-produced plasmas and laser-based plasma diagnostics has fueled interest in the formation of plasmas at densities nearing solid density. There are two separate areas where the proposed next generation sources can play a critical role in moving these fields substantially forward. The first is in the area of warm dense matter research, where X-ray Free Electron Lasers (XFEL) and the next generation of Heavy Ion Beam sources, will provide major improvements over the current state of the field. The second is in the area of techniques relevant to hot dense matter production and diagnostics, where the role of the 4<sup>th</sup> generation light sources, which are in this regard essentially x-ray lasers, will provide substantive improvements. For more information on these facilities see the website <http://www-ssrl.slac.stanford.edu/LCLS/> for information on the LCLS facility, the website <http://www-hasylab.desy.de/facility/fel/> for information on the TESLA facility and the TESLA Test Facility (TTF) a soft x-ray FEL facility), and the website [http://hifweb.lbl.gov/public/papers/US\\_accelerator\\_HEDP.12.pdf](http://hifweb.lbl.gov/public/papers/US_accelerator_HEDP.12.pdf) for information on the ion

beam sources. <http://www-aix.gsi.de/~plasma/> for information on the GSI ion beam sources

For the 4<sup>th</sup> generation sources, whether we are interested in creating warm dense matter, performing Thomson scattering, or probing a plasma the XFEL capability, will provide a major advance on any capability that exists with 3<sup>rd</sup> generation sources. The key to the advance is the tunable, narrow band x-ray source with very short pulse duration. Since the individual bunch photon intensity is the essential quantity for all the plasma-based research, comparing peak spectral brightness best summarizes the comparison of the XFEL to current synchrotron sources – see the Source Table in Fig. 18. Indeed, one finds an enhancement of 10 orders of magnitude will make the XFEL most promising source for plasma-based research. The utility of the high repetition rate of other sources, *e.g.*, APS or ESRF, are not useful here since we require a single photon pulse to either heat, scatter, or probe matter that is transient. Indeed, to create solid matter that is at a temperature greater than 1 eV temperature while not expanding on x-ray light sources will require the capability of the XFEL.

For the next generation of ion beam sources the high intensity upgrade of the heavy ion beam accelerator facilities will lead to energy densities greater than  $10^{11}$  ergs/cm<sup>3</sup> and temperatures between 1 and 10 eV at solid-state densities, enabling interesting experiments in the regime of non-ideal plasmas, *e.g.*, in the interior of the Jovian planet. (Tahir, 2001) These experiments are similar to those that may be performed on the 4<sup>th</sup> generation light sources; however, the energy will potentially provide heating of larger samples. This, then, will create WDM samples that have gradients that are small when compared to the size of the warmed volume. Further, the coupling of an intense short pulse laser source at the future heavy ion facility can provide an x-ray absorption source. It is important to point out that the approach taken here is quite distinct from that taken in the SIS-100 facility proposed for GSI, Darmstadt. In the GSI approach the ion beam heating is achieved by using substantially larger amounts of beam energy, with the beam passing through the sample before reaching the Bragg peak. This requires substantially larger facilities. In the approach proposed here we use the favorable energy deposition associated with the Bragg peak to enhanced energy transfer from the heavy ion beam to the sample. This will allow a more efficient coupling of the beam energy and permit the construction of a heavy ion beam facility in a more cost-effective manner

## A. Warm Dense Matter

With a short duration pulse containing a substantial number of high-energy photons or ions one can generate solid matter at temperatures of  $\leq 10$  eV, *i.e.*, warm dense matter. The interest in the warm dense matter regime arises because in dense plasmas the atoms and/or ions will start to behave in a manner that is intrinsically coupled to the plasma. That is, the plasma starts to exhibit long- and short-range order due to the correlating effects of the atoms/ions. This intriguing regime where the plasma can no longer be considered a thermal bath and the atoms are no longer well described by their isolated atom behavior provides a tremendous challenge to researchers. In the limit of dense cool plasmas one obviously arrives at the threshold of condensed matter. Here the problem has changed from a perturbative approach to ground-state methods where complete renormalization of the atom/ion and its environment is essential.

From the prospective of plasma studies the defining quantity is the coupling parameter  $\Gamma$ , *i.e.*, the ratio of the inter-atomic potential energy to the thermal energy given in Eq. 1:

$$\Gamma = \frac{Z^2 e^2}{r_0 k T} \quad \text{with} \quad r_0 = \left( \frac{3Z}{4n_e} \right)^{1/3} \quad 1)$$

here  $Z$  is the ion charge and  $r_0$  is the interparticle spacing given in terms of the electron density  $n_e$ . The regions of interest span the density-temperature phase space going from modestly coupled ( $\Gamma \leq 1$ ) to strongly coupled ( $\Gamma > 1$ ), while bridging the transition regimes between solid to liquid to plasma. This is schematically represented in Fig. 2 .

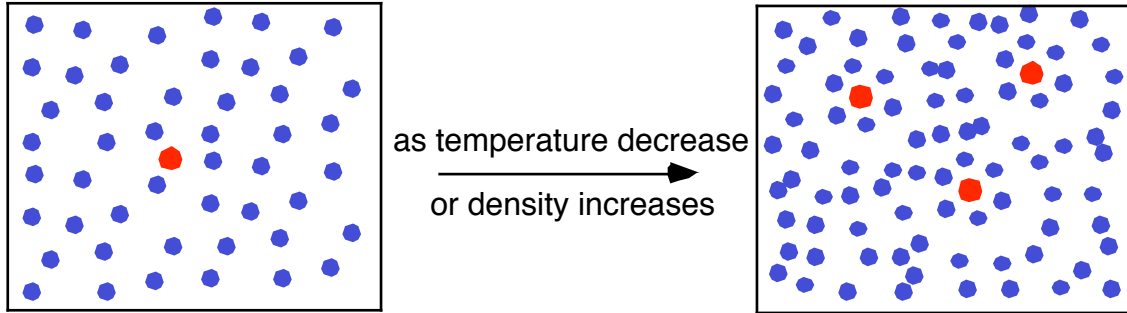


**Figure 2. Schematic of the effect of increasing the coupling parameter,  $\Gamma$ , in a plasma. As indicated in Eq. 1 the coupling will occur with increasing density and/or decreasing temperature.**

On the other hand, from the point of view of a solid the temperature of the system relative to its Fermi energy defines the WDM regime. The Fermi energy  $E_{\text{Fermi}}$  is the maximum energy level of an electron in cold (essentially  $T = 0$ ) condensed matter and thus when the temperature  $T \ll E_{\text{Fermi}} = T_{\text{Fermi}}$  then the standard tools of condensed matter are applicable. However, when the temperature  $T \geq T_{\text{Fermi}}$  one gets excitation of the core level and potentially ionization leading to a complex mixture of species. In this latter case the ion-electron correlations change and the ion-ion correlations yield distinct short and long-range order, when compared to the  $T = 0$  solid. This is illustrated in the Fig. 3 where we show for the case of aluminum the changes in the electronic density localization and the band structure of solid aluminum at  $T = 0$  and the band structure at finite  $T > T_{\text{Fermi}}$ . The calculation of the structure becomes substantially more complex due to the number of band required to describe the system and due to the fact that there are several ionization stages present.

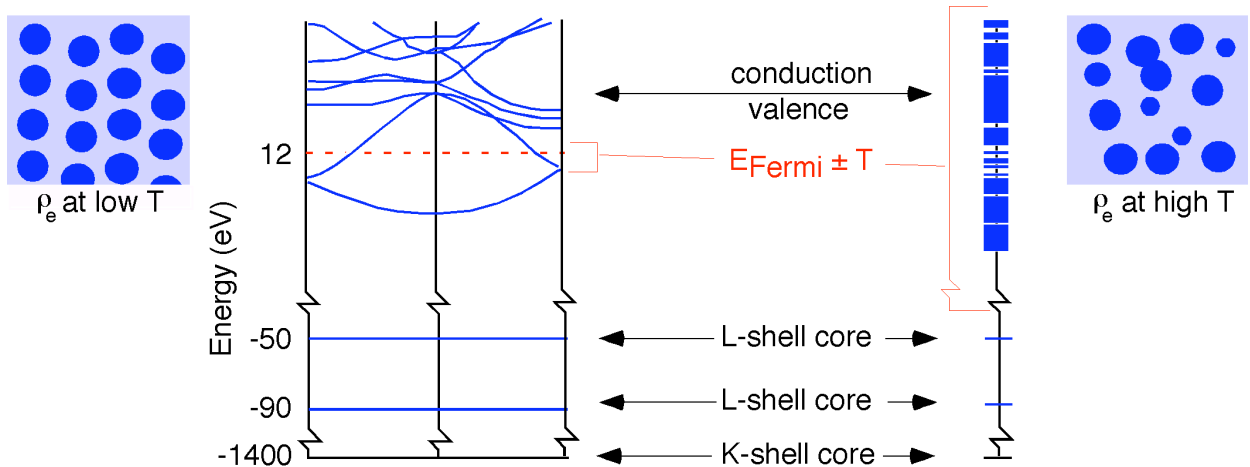


**Figure 3. The warm dense regime is defined from the point of view of condensed matter. The increase of the**

temperature toward the Fermi temperature while keeping the density at normal solid density creates a more complex band structure as well as numerous possibilities for more random placement of the electron charge density

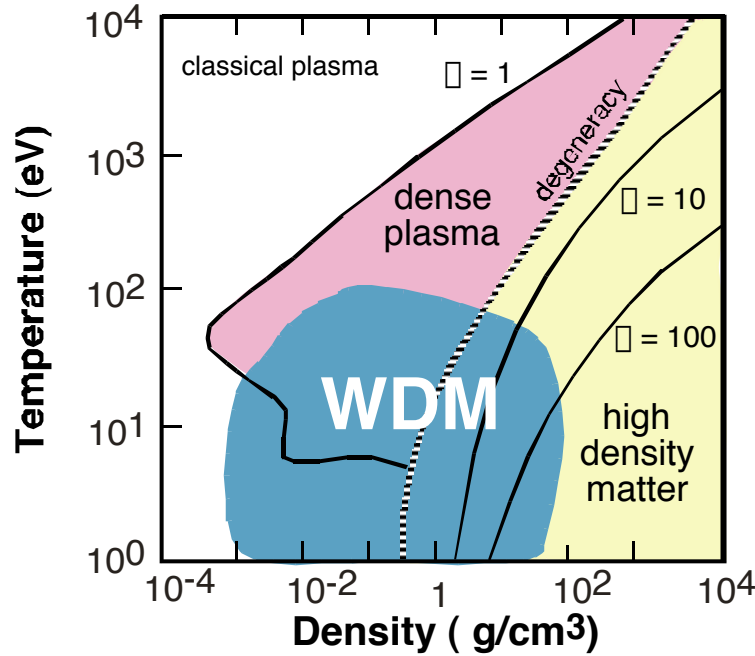


**Figure 4** The temperature-density phase diagram for aluminum. The relevant regimes are noted, as are the various values of the coupling  $\Gamma$ . The region of greatest uncertainty is roughly noted by the teal area. Also indicated is the region where degeneracy will become important: it is the region to the right of the line where the chemical potential  $\mu = 0$ . The aluminum data is derived from the QEOS formalism (More, 1988)

In Fig. 4 above we show the region of the temperature-density plane where warm dense matter studies are important. Here we show the temperature ( $T$ ) in eV versus the density ( $\rho$ ) in  $\text{g/cm}^3$  both for aluminum, a moderate  $Z$  element. The various values of the strong coupling parameter defined in Eq. 1 are shown as well as the region where degeneracy plays a role. The region where the theoretical uncertainties are largest are those where the standard theoretical approaches fail and experiments are exceedingly difficult; the WDM region indicates this. The difficulty arises theoretically from the fact that this is a regime where there are no obvious expansion parameters, as the usual perturbation expansions in small parameters used in plasma phase theories are no longer valid. Further, there becomes an increased importance on density-dependent effects, *e.g.*, pressure ionization, as the surroundings starts to impinge on the internal structure of the ion or atom. Experimentally the study of warm dense matter is difficult, as the isolation of samples in this regime is complicated. Indeed, although the plasma evolution of *every*  $\rho$ - $T$  path that starts from the solid phase goes through this regime and plays an important role in its evolution, trying to isolate warm dense matter remains a major challenge.

## B. Studying Warm Dense Matter in the Laboratory

It has been exceedingly difficult to perform experiments in the warm dense matter regime, which is, simply, why we know so little about it. As a first step, one must create a well-characterized warm dense matter state; the second is to gain information on the state through experiments. The first step has been the problem: warm dense matter is not a limiting case of matter, *e.g.*, high- or low-temperature. When created in a laboratory environment, it does not tend to remain in a specified thermodynamic state for very long, making characterization difficult. The various methods suggested to produce the kind of warm dense matter of interest are the proposed x-ray free electron laser, the heavy ion beams of interest here, and with a sub-30-fs visible laser pulse on sub-100-Å-thick foils and perform thermodynamic measurements on a few-fs timescale over extremely small spatial dimensions. As we will discuss the heavy ion beam approach presents a very interesting option.

One finds that the problem is not that WDM is difficult to create as it occurs widely; but, to create it in a manner that is conducive to quantitative examination. The problem is that the deposition of substantial energy in a short time leads to large gradients in both temperature and density. If the energy is deposited slowly so that hydrodynamics expansion dominates the system then the difficulties in isolating a well-defined state is further compounded. The effort in most WDM experiments to date has been in creating matter that can be diagnosed. Then diagnostics must define the state of the matter: there must be a measurement of the temperatures (ion, electron and radiation) and densities (the electron, ion and possibly the mass density); measurements of the pressure, flow velocities and the uniformity must be undertaken; and, one needs to consider the effect of shocks, turbulence, and material mixing. These requirements have been difficult to meet and indeed have been achieved in very few cases. One is attempting to measure the equation of state (EOS) of the system. The equation of state is a formula describing the relationship between various macroscopically measurable properties of a system, usually the temperature-density-pressure.

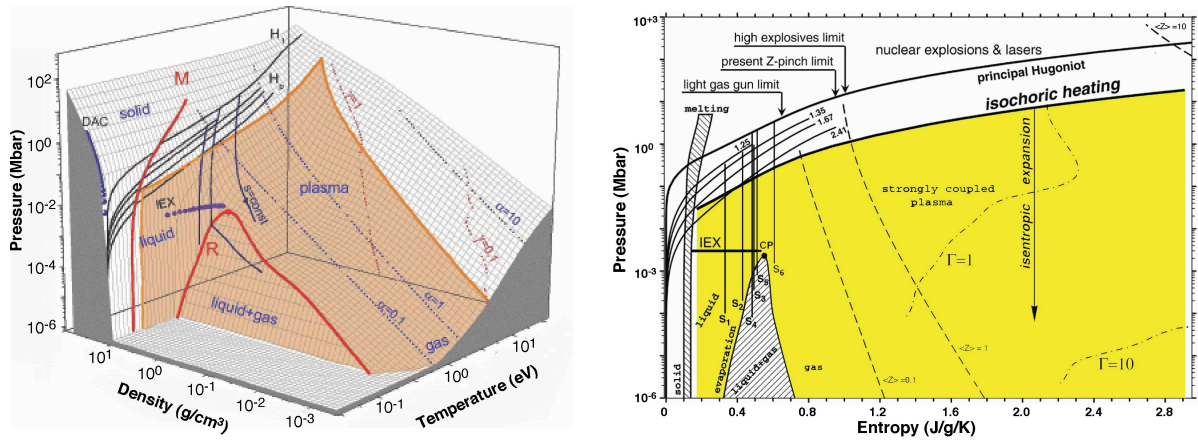


**Figure 5.** The phase-space diagram of Pb with experimental data and various phases. shown a) the Pressure-Density- Temperature phase diagram. b) The Pressure-Entropy diagram showing the isochoric heating/isentropic release curves.

The best examples of WDM studies performed to the level indicated are found in the literature on shock generation with the largest part of these coming from experiments employing single strong shocks. As an indication of the possibilities we show a phase diagram of lead, a much studied material, in Fig. 5 a and b. The Fig. 5a shows the pressure-density-temperature phase space with curves generated by difference experiments. The H<sub>i</sub> and H<sub>p</sub> are the shock Hugoniot for the principal and porous Pb. The Hugoniot is the locus of states reached by single strong shocks, one point for each shock. As is clear these Hugoniot represent the largest

contributions to the data set. The diamond anvil cell (DAC) measurement are done at very low temperature and form a limiting case not of interest to WDM studies. There is one isobaric expansion experiment (IEX). These represent the experiments in the region of interest, illustrating the paucity of data. The one additional curve that is shown is noted as by  $s=\text{const}$  and represents the isochoric, constant density, heating of a sample and the isentropic, constant entropy (S), release. Indeed, the ion-beams capability will attempt to access this regime by providing uniform bulk heating and then isentropic expansion. This is shown in Fig. 5b where the phase space representation has been converted to Pressure-Entropy space. In Fig 5b the same experiments are shown as on Fig. 5a with the isochoric heating/isentropic expansion more clearly indicated.

The understanding to be gleaned from Fig 5 is that there are: 1) little data in the WDM, even for a well studied material; 2) there are few extant methods that can access the regime of interest, and 3) the potential of volumetric heating possible with heavy ion beams can play an important role. Indeed the concept for ion-beam heating is straightforward and is illustrated in Fig. 6

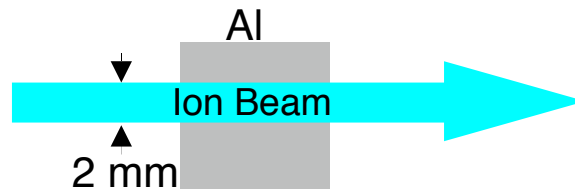


**Figure 6. Schematic of the ion beam heating experiment**

Figure 6 schematically illustrates an experiment of this nature. The Al phase diagram of Fig 4 illustrates the parameter space of such an experiment. In Fig. 7 the phase space diagram has been annotated, to show the trajectory of the isochoric heating and the subsequent release along the isentrope, by red and pink lines, respectively. Note that the entire trajectory maps out a set of states in the WDM regime that, if each of those states is in thermodynamic equilibrium, provide a large set of data. Further, the use of a foam or porous target, indicated by the trajectory displaced to lower than normal solid density allows one to collect data across a wide swath of the WDM region.

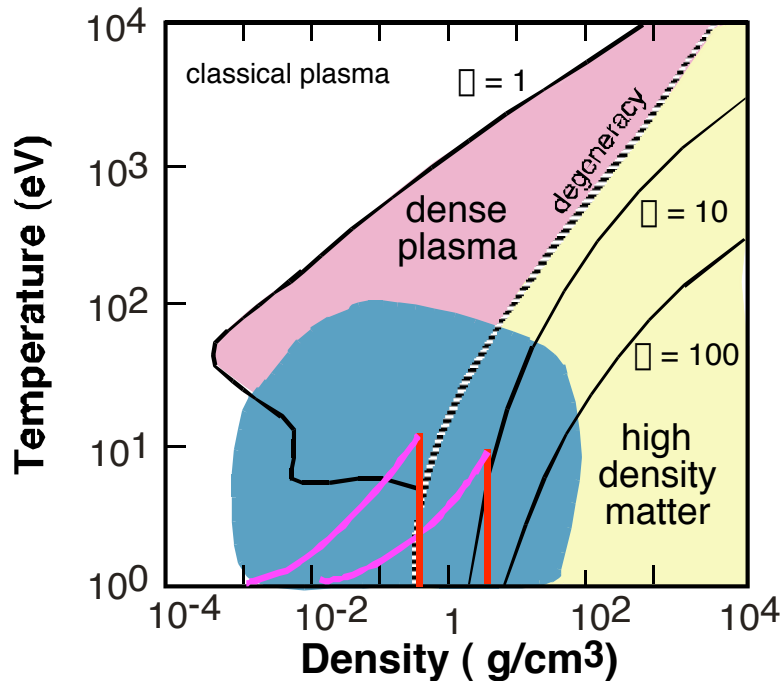




**Figure 7 The temperature-density phase diagram for aluminum. As Fig. 4 with the inclusion of the schematic isochoric heating (red) trajectory and the subsequent isentropic (pink) trajectory. Note that underdense material, e.g., foams, allows multiple trajectories to be studied.**

### III. Current State WDM studies

In the past few methods have been used to study the WDM regime, as indicated by the discussion above; however, currently more experimental techniques are being employed. We will attempt to outline the state of the art specific to WDM studies. The methods we will cover include experiments using Short pulse Laser experiments in their various forms, High-energy lasers, 3<sup>rd</sup> generation light sources, and large and small pulse power machines. The main purpose is to provide an understanding of the fact that although an ion beam facility does not exist the field is far from crowded with viable options.

#### A) Short pulse lasers

Over the past few decades as visible laser have become prevalent the number of application to the production of exotic states of matter have increased. More recently the move toward ever shorter pulse lasers systems have made for exciting new possibilities in the generation of these novel states. However, the number of experiments directed toward studies of the detailed nature of either HDM or WDM is quite small. The overarching reason for this paucity of experiments is the difficulty faced when one has a visible laser and attempts to directly heat dense matter, as the visible laser can not penetrate effectively beyond the critical electron density, which as function of the laser wavelength,  $\lambda_{\text{laser}}$  (Ångstroms), given by

$$n_{\text{critical}} \approx 10^{29} / \lambda_{\text{laser}}^2 \text{ (cm}^{-3}\text{)} \quad 2)$$

This indicates that the primary interaction of the short pulse laser will be with a region of small depth,  $\leq 1000 \text{ Å}$ , and leads to substantial gradient formation on the time scales of the laser irradiation, which lead to hot dens plasma studies. This is the case for the overwhelming majority of laser-matter experiments to date. In contrast to this are two examples of potentially interesting experimental setups that could lead to WDM matter experimental interest.

The first type of experiment uses of a short pulse laser with diagnostic capability to record information on the state of the heated system on the time scale of the laser irradiation (Widmann et PRL 92, 125002 (2004)). The concept is shown schematically in Fig. 8 where the short pulse laser is split into a beam that will be converted to 2 $\omega$  to heat the target and one that will be used as a probe. The part to be used as a probe is put through a Michelson interferometric setup. The resultant two probe beams impinge on the sample surface, one before the heating beam arrives and one after, and are afterwards recombined in a spectrometer creating a one-dimensional image of the surface at various times relative to the heating pulse. This information about the surface motion together with the energy of the incident, reflected, scattered and transmitted beams provides a best effort to date at bracketing the equation of state.



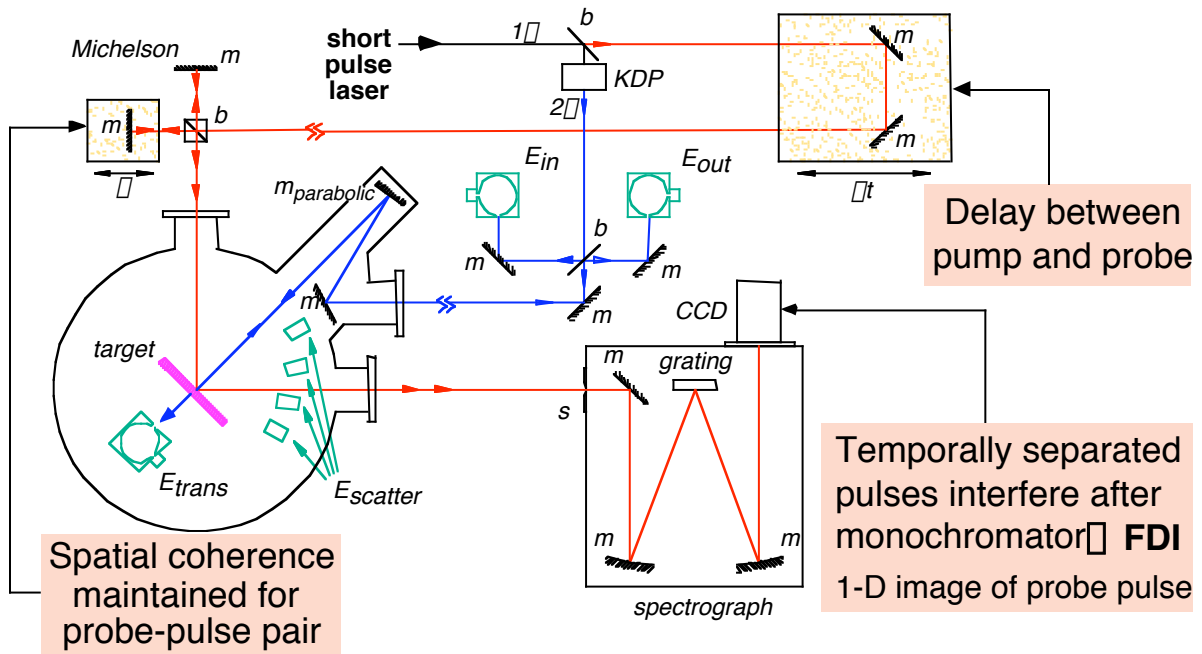


**Figure 8.** Set up of a short pulse laser experiment to measure the states of a heated sample as a function of time.

The results from this experimental setup have proved interesting but there remains the problem the sample is undergoing hydrodynamic motion and has substantial gradients during the time of the experiments. The lack of sample uniformity cannot be ameliorated due to the fact that the heating occurs non-uniformly.

The second type of experiment would be quite similar to the one shown in Fig. 8 except one would use a slightly longer pulse and overcoat the thin sample with a large layer of lower  $Z$  material (Davidson et al., JQSRT, **65**, 151 (2000)). For example, one could have a 100 Å layer of Fe embedded in a sandwiched configuration with 1500 Å of CH on either side. The object would be to heat the Fe layer via electron conduction from the laser irradiated surfaces and wait until the Fe layer was uniform. This would, were simulations to prove correct, form a very uniform Fe layer at times long compared to the laser pulse. The simulations show, in Fig. 9, that at 5 ps, the Fe sample is at 0.2 of normal density and at an elevated temperature of 150 eV. This, if true, would allow one to study the WDM regime also.

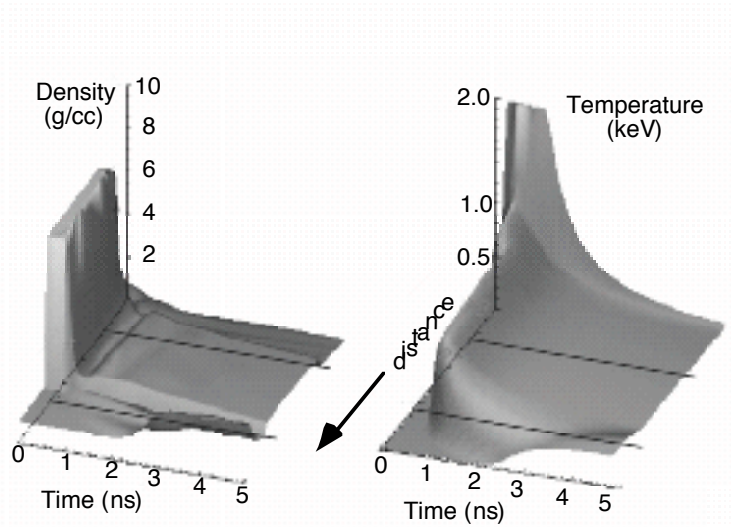


**Figure 9.** A simulation showing the temperature and density history of a one dimensional sample irradiated

from the far side with a 700 ps short pulse laser at  $10^{17}$  W/cm<sup>2</sup>. The sample starts as a 100 Å Fe layer sandwiched between 1500 Å of CH.

The fact that this experiment has never been performed may be due to one or more of several factors. Two of these factors are: 1) Simulations are more alluring than the experimental program needed to achieve them; 2) The interest in creating a test bed for WDM using a higher energy short pulse laser is of low priority compared to the number of exotic states that can be produced more simply.

## B. 3<sup>rd</sup> Generation X-ray Light Sources

Experiments on current x-ray light sources are limited by the fact that these light sources have low intensity per bunch and have relatively long pulse durations,  $\geq 50$  ps. Thus to study WDM states one needs to couple a short pulse laser as a heating source with a beamline at the light source. This has been done at the Advanced Light Source, Advanced Photon Source, and the European Synchrotron Radiation Facility. At all these sources similar experiments have been performed which are schematically illustrated in Fig. 10. The basic idea is to use the short pulse laser to create a perturbation at a crystal surface and use the x-rays from the light source to probe the disturbance. The experiments have proved extremely fruitful but are limited by the fact that signal levels per bunch are small so that the perturbed sample must be probed repeatedly to gather data. This is overcome by ensuring that the sample perturbation is small so that the crystal returns to its original state between pulses, which with current technology is limited by the short pulse laser repetition rate of  $\sim 1$  kHz. An example of the results is shown on the right-hand side of the Fig. 10 where the diffracted signal is shown as a function of time after the short-pulse laser perturbation. This form of data has been used to measure the phonon dispersion relations under non-equilibrium conditions, providing a measure of the electron-phonon coupling, and observation of order-disorder laser-induced phase transitions.

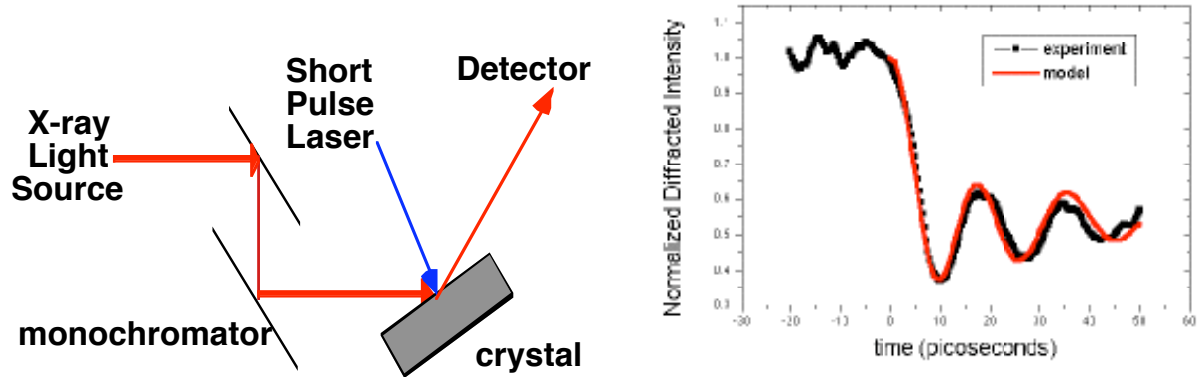


Figure 10. The left-hand side shows a schematic of the short pulse laser coupled to a 3<sup>rd</sup> generation x-ray light source. The laser is synchronized to the RF signal from the light source to provide  $\sim 1$  ps timing. The time resolution of the experiment depends on the detector as the light source has  $\geq 50$  ps time duration. The right-hand side shows the diffracted signal as a function of time measured from the laser irradiation.

## C. High-Energy Lasers

The use of high energy lasers -for the purposes of discussion here we take laser with energies greater than  $> 50$  J- to produce WDM is predominantly associated with using the high energy laser to drive a strong shock for the purposes of using the Hugoniot relations to measure the equation of state along the principle single shock Hugoniot (see for example: L. B. Da Silva et al., Phys. Rev. Lett. **78**, 483 (1997); and, G. W. Collins et al., Phys. Plasmas **5**, 1864 (1998)). Next, one finds that in the run-in phase of a radiatively driven inertial fusion capsule implosion

the desire to remain on a low adiabat leads to WDM conditions. Although this is not a case where fundamental measurements can be made concerning the WDM state one could ideally use the detailed measurement of the hydrodynamics of the run-in to infer the state of the imploding capsule. Finally, we show the one set of experiments performed on high-energy lasers where the laser provides an x-ray source to warm matter and also provides an x-ray source that allows the probing of the warmed matter by Thomson Scattering.

The use of the high-energy laser to create shocks has been perfected over the past decade and provides a method of reaching very high pressures ( $\geq 10$  Mbar) in the laboratory. The schematic is straightforward and shown in Figure 11 together with the data where the image of the shock and the pusher interfaces are shown as a function of time. The latter data provides the pusher and shock velocities that together with the Hugoniot relations provide the equation of state for the shock pressure induced by the laser.

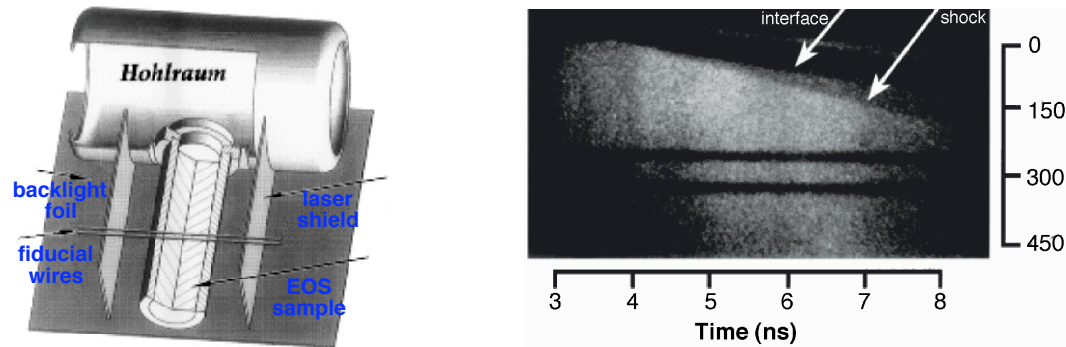


Figure 11. The use of a hohlraum, left-hand side, an enclosure that is irradiated by a high-energy laser to convert the visible light to x-ray that then drive a shock into the sample appended. Another laser beam impinges on the backlight foil to create a long duration x-ray source to observe the shock transit. This is imaged on a x-ray streak camera and produces, right-hand side, a record of the shock and pusher positions as a function of time.

The result of each of these experiments is a point on the Hugoniot an example of which is shown in Fig. 12 where several sets of experimental data are shown.

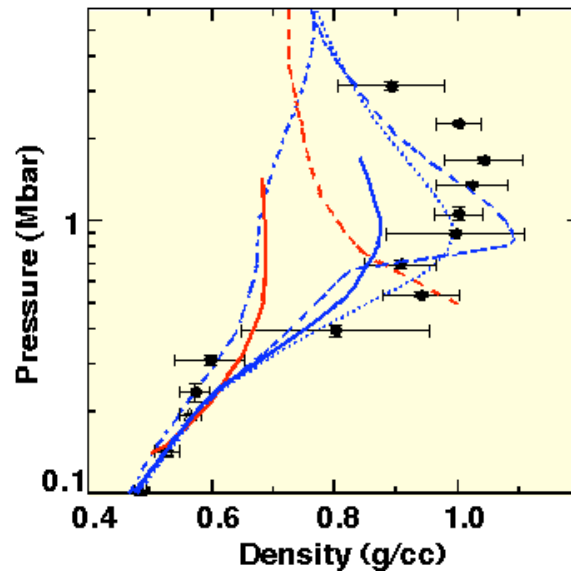
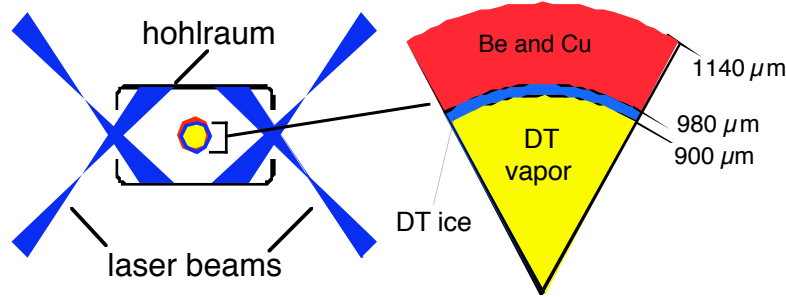
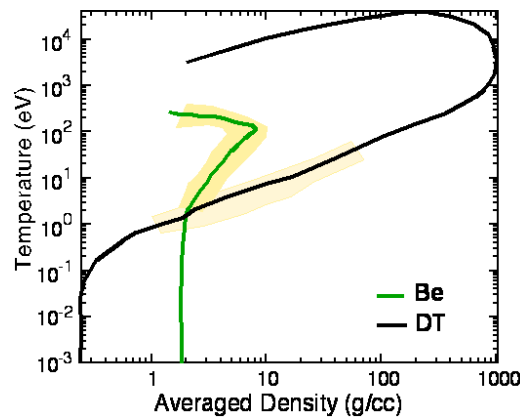


Figure 12. Gas gun data (triangles) are shown. The blue curve indicate models based on fits to extant data while the red line are physical model base on *ab initio* methods. The EOS model is shown as the dotted blue line. The widely used SESAME tabular EOS is shown as a dot-dashed blue line. The remaining curves are newer attempts to model the data.

The accessing of the WDM regime occurs much more frequently as an integral part of experiment where the end result is some aspect of the HDM regime. One excellent example of this is the run-in phase of indirectly driven inertial fusion capsules. To best keep the pressure of the inflowing material at low pressures one designs the driving pulse to keep the pusher (shell of the capsule) on a low adiabat. This then allows the pusher to compress the gas (fuel inside the capsule) more efficiently. In Fig. 13, the schematic configuration of the experiment is shown. On the left-hand side is the radiation enclosure, hohlraum, into which laser beams are focused. The lasers impinge on the high-Z wall and through laser-matter interaction the laser light is converted to x-rays that then irradiate the capsule in the center of the hohlraum. The capsule is shown in diameter on the right-hand side where the pusher is composed of Cu, to block the x-ray from heating the DT fuel, and Be. The simulated temperature-density paths for a representative volume of the Be pusher and the volume of the DT fuel are shown in Fig. 14 where we see that for large parts of the run-in the fuel and the pusher are in the WDM regime. The light yellow areas indicate the WDM regime. Detailed diagnosis of the WDM, in a configuration as complex as this, is beyond the current scope of any experimental program. However, the hydrodynamics of an experiment of this kind can be measured, e.g., the timing of the shocks and the imaging of the compressing core, and that would provide indirect evidence of the WDM models used in the simulations.



**Figure 13.** Schematic of the indirectly driven ICF capsule experiment on the left and an enlarged view of the capsule, right, showing the pusher and the fuel regions



**Figure 14.** Temperature and density track of representative regions of the pusher and the fuel are shown in green and black, respectively. The yellow highlighting indicates the WDM regime. Further, the fuel can be seen reaching extreme condition, e.g., 1000 g/cc and  $10^4$  eV at peak compression.

Finally, there is one particular experiment on high-energy lasers where the main focus is the WDM regime. In Fig. 15 we see on the left the target configuration: here a plug of Be surrounded by a Rh layer. The Rh layer is irradiated with 15 laser beams to create x-rays that heat the sample. These beams are 1 ns in duration and after they turn off 30 beams irradiate the Ti layer to create x-ray from the He-like Ti resonance lines that are then pass through the heated Be. The Ti x-rays are scattered from the heated Be sample and recorded on a spectrometer. The

Compton shifted scattering, shown in the data on the right-hand side, as the green area represent the free electrons scattering from the Be sample. The lower plot shows the measurement with no x-ray heating beams and represents the  $T = 0$  case. The upper curve shows that the number of free electrons per Be atom,  $z_f$ , increases due to the heating. The sensitivity of the measurement of the temperature using this technique is quite accurate with differences in 10 eV easily discernible.

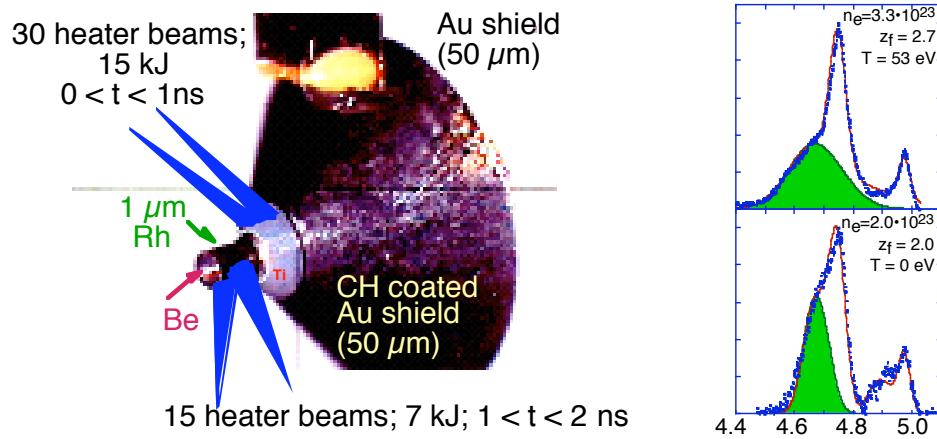


**Figure 15.** On the right target configuration of a high energy laser experiment specifically design to create and probe the WDM regime. The experiment has 15 beams creating an x-ray source that heats a Be sample, and 30 beams that create an x-ray probes to be scattered from the heated sample. The Thomson Scattering signal is on the right with the green area indicating the unbound electrons contribution. The bottom right plot show the data with no heating and the top shows the data from a sample that is heated.

## D. Large Pulse Power Technology

The recent improvements in efficiently delivering the vast amounts of energy generated by pulsed power technology to loads have created an important avenue for research into the generation of WDM via shocks. The researchers at the Sandia Z facility have perfected a technique to launch cold, high velocity (to 28 km/s) flyer plates and have obtained results at 1-Mbar in  $D_2$ . The effort began in the year 2000 with results in the 0.3-0.8 Mbar range reached in 2001. Shown in Fig. 16, the pressure and density relationship (shock Hugoniot) agrees with the SESAME EOS model (used in most hydrodynamics simulation codes) and with *ab initio* molecular dynamics calculations, but disagrees with the greater compressibility in Nova data and the Ross model (see Fig. 12). These data contribute to the controversy about the  $D_2$  data and have implications for inertial confinement fusion (ICF) and for stellar and planetary models. The fact that there is a disagreement is not of immediate importance here; however, it brings two important points to the forefront: 1) There is in the study of new regimes a real need for alternative methods to perform experiments in the same parts of phase space and 2) the large energy of the new pulse power machine will be an important resource in the future for the study of WDM. Indeed, the relatively new interest in the WDM regime should spark this interest.

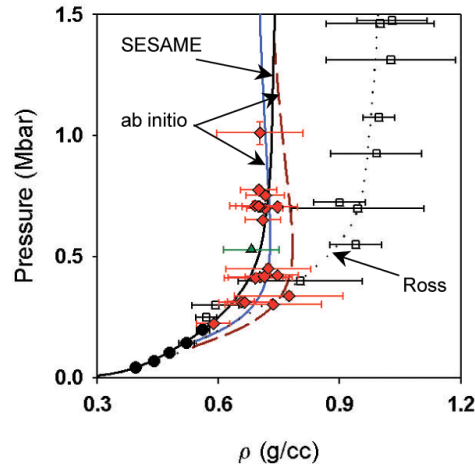


**Figure 16.** EOS data from the Z Pulsed Power machine (red diamonds), gas gun (solid circles), and Nova (open squares) data for  $D_2$  compared with *ab initio* calculations and the SESAME and Ross models. The disagreement with the laser-based shock Hugoniot data remains a subject of discussion (See Fig. 12 for reference)

### E. Smaller Pulse Power Technology

Due to the rather low temperatures that are of interest to the WDM regime it is not surprising to find that alternative methods using relatively simple pulse power plasma generators have made inroads into the stuff of WDM. In these examples presented here measurements are made of a transport property that are of interest in the WDM regime. However, there are no direct measurement of both the temperature and density of the system. These conditions tend to be inferred by plausibility arguments and/or simulations. Indeed the experimental setups are modest, at least by the usual high-energy laser facility or large pulsed power facility standards and efforts to perfect the methods may prove cost-effective.

All these pulsed power concepts are variations of exploding/evaporating wires with the added feature of tamping the wires in various ways to retain the density. First, there is the work of Benage et al. (Phys. Rev. Lett. **83**, 2953 (1999)) in which the electrical transport properties of dense aluminum are measured in the disordered liquid-like phase using a well-tamped, thermally equilibrated, exploding wire  $z$  pinch. Direct measurements of the electrical conductivity were made using voltage and current measurements. These measurements span the minimum conductivity regime and found generally good agreement with theory, in contrast to other experiments performed in similar regimes that indicated poor agreement. Here the range of ion densities and temperatures inferred were from  $n_i \sim 5.1 \times 10^{22} \text{ cm}^{-3}$  at  $T \sim 0.85 \text{ eV}$  to  $n_i \sim 1.5 \times 10^{21} \text{ cm}^{-3}$  at  $T \sim 25 \text{ eV}$ , with strong coupling values  $\Gamma_{ii}$  from 15 to 2. Krisch and Kunze (Phys Rev. E **58**, 6557 (1998)) also studied aluminum wires rapidly vaporized in small glass capillaries by means of a short pulse current from an electrical discharge converting the aluminum into a non-ideal plasma at high density. For a short period of time, the inner wall of the rigid glass capillary confines the homogeneous plasma until the induced pressure pulse disintegrates the capillary. During this part of the discharge, no instabilities occur, and the transient plasma covers a range of inferred conditions: the density ranges from 0.001 to 1.0  $\text{g/cm}^3$ , the temperature from 0.6 to 2.1 eV and the electron density from  $2 \times 10^{18}$  to  $3 \times 10^{19} \text{ cm}^{-3}$ . Plasma conductivity was deduced by simply applying Ohm's law to the measured voltage drop across the wire and to the measured current through the wire. On the other hand, DeSilva and Katsouras (Phys Rev. E **57**, 5945 (1998)) measured of electrical conductivity of copper and aluminum plasmas in the temperature range 0.85-2.6 eV with densities from 0.3 to 0.02  $\text{g/cm}^3$ . Plasmas were created by rapid vaporization of metal wires in a water bath. At temperatures below about 1.3 eV, as density decreases from the highest values measured, the conductivity falls roughly as the cube of density,



reaches a minimum, and subsequently rises to approach the Spitzer prediction at low density. Finally, in the work of Renaudin et al. (Phys. Rev. Lett. **88**, 215001 (2002)) the electrical resistivity, pressure, and internal energy variation of warm dense titanium (density  $0.2 \text{ g/cm}^3$ ) and aluminum (density  $0.1 \text{ g/cm}^3$ ) are measured inside a closed-vessel. The temperature range, which is inferred from equation of state tables, varies from 1.3 to 2.6 eV, and it is assumed that the vaporized wire is homogeneous and thermally equilibrated.

## IV. The Near Future

In the next five years there will be few new capabilities that come on line to address the physics of the WDM regime. These fall into three broad categories: the upgrading of existing facilities to include intense short pulse laser systems, in particular the addition of petawatt lasers; the implementation of a sub-picosecond on a 3<sup>rd</sup> generation x-ray sources light sources; and, the first 4<sup>th</sup> generation x-ray light source, a free electron laser will open.

### A. Petawatt lasers as Facility Upgrades

Since the primary interaction with optical lasers is limited to the surfaces due to the limitation to the propagation of light to electron densities  $\ll n_{cr}$  (see Eq. 2) we find that there is an keen interest in having very high intensity laser system associated with large scale facilities to provide a method of probing the HED matter that is produced. Further, in stand-alone configuration the petawatt laser may provide a source of intriguing plasma generation mechanism as well as being able to produce intense protons beams that have durations of  $\sim 5 \text{ ps}$ . The number of facilities proposed and funded petawatt lasers is substantial and the map of lasers in the US on a graph of laser energy versus pulse duration is presented in Fig. 17.

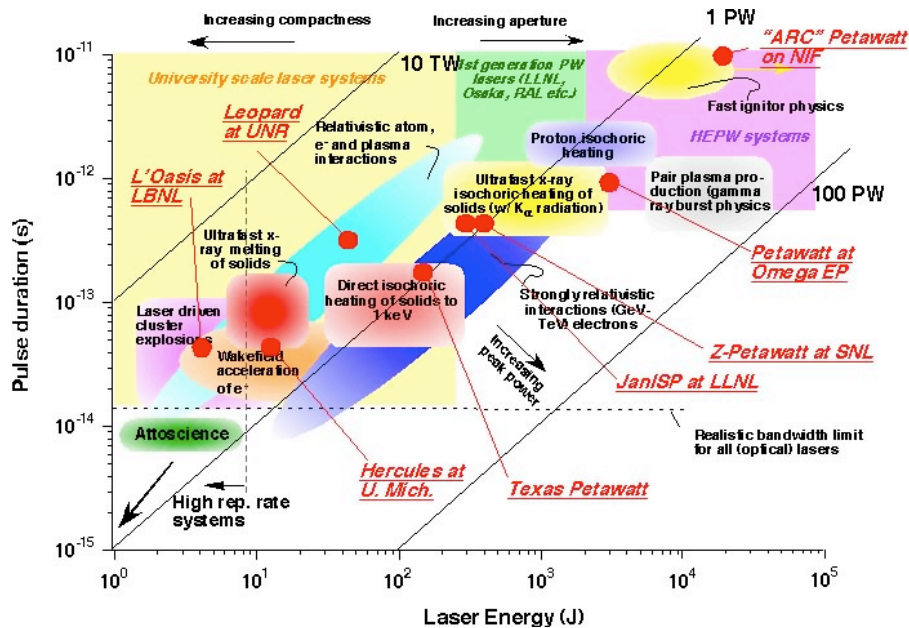


Figure 17. Laser capabilities in the USA. The various facilities are called out in red on a graph of Laser energy in Joules versus pulse duration in seconds. The Petawatt systems at Omega EP, Z-Petawatt, and ARC all have as a central application the generation of short pulse intense x-rays for probing the dense matter generated. The facility Jan/SP is functioning currently and producing proton beam for various purpose.

The wealth of facilities and those that will come on line within the next few years indicate the interest in the use of petawatt systems. However, these are largely not devoted to WDM studies. Meanwhile at the Jan/SP facility intense short pulses (5 ps) of protons have been reported and there will clear be progress in the effort to develop this source for WDM matter studies in the near future.



## B. Subpicosecond 3<sup>rd</sup> generation X-ray Light sources

There are two possible venues where sub-picosecond x-ray light sources can be used. The first is the SPPS (Short Pulse Photon Source) in operation at SSRL and second is the “Slicing Source” at the ALS (Advanced Light Source) to be in operation in 2005 at LBNL. The SPPS as can be seen from the Source Table in Fig. 18 is in operation; however, SPPS will have a short life as the LCLS facility construction will require its space. With particular respect to the 3<sup>rd</sup> generation sources the study of WDM will be restricted predominantly to the type of experiments that have already been performed, see section III.B.

	SPPS (SSRL)	Slicing (ALS)	VUV-FEL (DESY)	LCLS (SSRL)
Energy range (keV)	8	0.2-10	0.04- 0.2	0.08 8.0
Photons/pulse/0.1%BW	$1 \times 10^8$	$8 \times 10^2$	$2 \times 10^{12}$	$2 \times 10^{12}$
Pulse length (fs)	80	200	50	100
Bandwidth (%)	0.1	0.1	0.3	0.3
Repetition rate (Hz)	10	$4 \times 10^4$	50	120
Start date	2004	2005	2005	2009

Figure 18. The newer X-ray Light Sources that could play a role in WDM research in the near future.

## C. Subpicosecond 4<sup>th</sup> generation X-ray Light sources

The advent of free-electron laser source should provide an important advance for WDM, and also HDM, research. These new light sources are laser-like in that there are high intense, small bandwidth, short pulses and they will be tunable. As such the first of these to start, the VUV-FEL at DESY (see the Source Table in Fig. 18) will allow studies of the interaction of laser and matter where the laser penetration will go beyond the surface, see Eq. 2. These sources are to be used for a series of experiment starting in 2005 that will assist in the understanding of the WDM matter regime. They include: The creation of WDM and the measurement of the equation of state of the matter; absorption spectroscopy of laser heated matter, and surface studies of femtosecond irradiated material.

## V. The Future

It is beyond the next four or five years that the capabilities of several facilities will come to fruition. The facility can be simply grouped into large-scale lasers –the National Ignition Facility (NIF at LLNL), and the petawatt enhancement to the Omega Laser (Omega EP at LLE)–, the up grade to the Z Pulsed Power Facility (ZR at Sandia), and the first x-ray Free electron laser (LCLS at SSRL). Each of these facilities will have related capabilities build up overseas. The potential for discovery becomes enormous particularly in a field as fertile at that of WDM. It is worth noting that of all these new facilities the only one that is dedicated to scientific use is the LCLS. All the other facilities are devoted largely to programmatic use and have small amounts (~10%) of their experimental time dedicated to users

However, the one capability that is missing is heavy ion beams. The SIS100 upgrade (proposed at GSI, Darmstadt) will be an important advance but will not come online until well after 2010. Thus, the prospect for volumetric and shockless heating using heavy ion beams is not on the horizon.

## VI. Advantages of the Ion Beam Approach

In summary it would appear that the development of a Heavy Ion Beam user capability would be timely. The case is clear that the heavy ion beams would provide a unique method to study HED matter as the heating will occur in a shockless manner, so that the creation of high pressures will be done in manner that is alternative to the standard approaches. Further, the long time scales and larger volumes obtainable will be unique for the WDM regime. In addition, the heating can be achieved by deposition at the Bragg range or shorter distances thus changing the deposition process. We can summarize the advantages of using the heavy ion beam approach by highlighting them here. First, the ion beams will be able to heat matter on a shockless manner, which is distinct from other approaches. This will permit distinct experimental techniques to access states in the WDM regime, a necessary condition for independent evaluation of both transport properties and the equations of state. Second, the state reached is achieved by volumetric energy deposition providing several related benefits: sample heating uniformity within a few percent; relatively large volumes essential for diagnostic access; reduced gradients within the sample; and, access to high entropy matter at high density. Third, the nature of the ion beams will lead to time scales that are long enough for equilibrium conditions to be established. Fourth, the ion beams parameters can be precisely controlled to provide variations in sample conditions and these beam parameters are measurable.

The basic configuration of the experiment is shown in Fig.6 is straightforward but does not represent the complexity necessary for the fielding of the experiment. There are several areas where the discussion above provides insight into the technical requirements for the experiment. First, it is clear that *in situ* measurement of the heated matter is essential. The probing of a warmed solid will require x-ray sources with duration shorter than the heavy ion beam source. In fact, the ideal situation would be to have an absorption source, i.e., a backlight, be sufficiently short in duration so that the changes in the state of the matter are extremely small. Currently the most efficient manner to produce intense short-pulse x-rays is with a high intensity,  $\geq 10$  TW, short pulse laser. Indeed coupling a short pulse laser to the ion beam capability will allow the x-ray probe to provide data that is essentially static. Thus, the coupling of a heavy ion beam facility with an intense short pulse laser capability is appropriate. Further, there are additional advantages to the coupling of the short pulse laser and the heavy ion beam, e.g., the laser can provide the sample pre-ionization so that the heavy ion beam can be used in dense finite temperature plasma-related studies

The simultaneous measurement of a set of physical parameters in an experiment where all the data must be obtained on each pulse necessitates the implementation of numerous diagnostics. This implementation, in turn, requires that the samples be fabricated in a manner that allows diagnostic access and that precise measurements are performed to define the sample characteristics. This is essential to ensure that each aspect of the experiment (beam deposition, spectrometers, time resolved radiography, *in situ* scattering and/or absorption measurements) can obtain uncompromised data. This will, in turn, necessitate that shielding of the various components of the sample as an integral part of the preparation. Next, the accuracy required for equation of state measurements is highly dependent on the measurement of, for example, the expansion velocities that in turn are dependent on accurate distance versus time diagnostics. In those cases where one uses x-radiography to measure the expansion uniformity of the sample, alignment and diagnostic calibration (e.g., in a streak camera this translates to the uncertainty in the sweep speed and its linearity) combine to make 10% accuracies difficult to attain. Third, the variation of the heavy ion beam focus, the variation in beam total energy, and the variation in the

beam spectrum (in heavy ion beam experiments this translates to details of the velocity profile) requires that one be able to generate a series of reproducible experiments to evaluate a single data point in the equation of state. Fourth, the need for reproducibility requires additional pulses. All these considerations lead to an estimated repetition rate for the heavy ion beam that is on the order of a minute. This repetition rate will be needed to account for the experiment preparations, calibrations, and accelerator variability.

## **VII. Conclusion**

In conclusion the unique aspects of shockless and volumetric heating, long duration pulses, and a user facility dedicated to the study of intriguing area of warm dense matter with heavy ion beams makes a five year plan an aggressive competitor with other planned and extant facilities.